

Food web reconstruction through phylogenetic transfer of low-rank network representation

Tanya Strydom^{1,2,‡} Salomé Bouskila^{1,‡} Francis Banville^{1,3,2} Ceres Barros⁴ Dominique Caron^{5,2}
Maxwell J Farrell⁶ Marie-Josée Fortin⁶ Victoria Hemming⁷ Benjamin Mercier^{3,2} Laura
J. Pollock^{5,2} Rogini Runghen⁸ Giulio V. Dalla Riva⁹ Timothée Poisot^{1,2}

¹ Département de Sciences Biologiques, Université de Montréal, Montréal, Canada ² Quebec Centre for Biodiversity Science, Montréal, Canada ³ Département de Biologie, Université de Sherbrooke, Sherbrooke, Canada ⁴ Department of Forest Resources Management, University of British Columbia, Vancouver, B.C., Canada ⁵ Department of Biology, McGill University, Montréal, Canada ⁶ Department of Ecology & Evolutionary Biology, University of Toronto, Toronto, Canada ⁷ Department of Forest and Conservation Sciences, University of British Columbia, Vancouver, Canada ⁸ Centre for Integrative Ecology, School of Biological Sciences, University of Canterbury, Canterbury, New Zealand ⁹ School of Mathematics and Statistics, University of Canterbury, Canterbury, New Zealand

‡ These authors contributed equally to the work

Correspondance to:

Timothée Poisot — timothee.poisot@umontreal.ca

1. Despite their importance in many ecological processes, collecting data and information on ecological interactions is an exceedingly challenging task. For this reason, large parts of the world have a data deficit when it comes to species interactions, and how the resulting networks are structured. As data collection alone is unlikely to be sufficient, community ecologists must adopt predictive methods.
2. We present a methodological framework that uses graph embedding and transfer learning to assemble a predicted list of trophic interactions of a species pool for which their interactions are unknown. Specifically, we ‘learn’ the information (latent traits) of species from a known interaction network and infer the latent traits of another species pool for which we have no *a priori* interaction data based on their phylogenetic relatedness to species from the known network. The latent traits can then be used to predict interactions and construct an interaction network.
3. Here we assembled a metaweb for Canadian mammals derived from interactions in the European food web, despite only 4% of common species being shared between the two locations. The results of the predictive model are compared against databases of recorded pairwise interactions, showing that we correctly recover 91% of known interactions.
4. The framework itself is robust even when the known network is incomplete or contains spurious interactions making it an ideal candidate as a tool for filling gaps when it comes to species interactions. We provide guidance on how this framework can be adapted by substituting some approaches or predictors in order to make it more generally applicable.

1 Introduction

2 There are two core challenges we are faced with in furthering our understanding of ecological networks
3 across space, particularly at macro-ecologically relevant scales (*e.g.* Trøjelsgaard & Olesen, 2016). First,
4 ecological networks within a location are difficult to sample properly (Jordano, 2016a, 2016b), resulting in
5 a widespread “Eltonian shortfall” (Hortal et al., 2015), *i.e.* a lack of knowledge about inter- and intra-
6 specific relationships. This first challenge has been, in large part, addressed by the recent emergence of a
7 suite of methods aiming to predict interactions within *existing* networks, many of which are reviewed in
8 Strydom, Catchen, et al. (2021). Second, recent analyses based on collected data (Poisot, Bergeron, et al.,
9 2021) or metadata (Cameron et al., 2019) highlight that ecological networks are currently studied in a
10 biased subset of space and bioclimates, which impedes our ability to generalize any local understanding of
11 network structure. Meaning that, although the framework to address incompleteness *within* networks
12 exists, there would still be regions for which, due to a *lack* of local interaction data, we are unable to infer
13 potential species interactions.

14 Here, we present a general method to infer potential trophic interactions, relying on the transfer learning
15 of network representations, specifically by using similarities of species in a biologically/ecologically
16 relevant proxy space (*e.g.* shared morphology or ancestry). Transfer learning is a machine learning
17 methodology that uses the knowledge gained from solving one problem and applying it to a related
18 (destination) problem (Pan & Yang, 2010; Torrey & Shavlik, 2010). In this instance, we solve the problem
19 of predicting trophic interactions between species, based on knowledge extracted from another species
20 pool for which interactions are known by using phylogenetic structure as a medium for transfer. There is a
21 plurality of measures of species similarities that can be used for inferring *potential* species interactions *i.e.*
22 metaweb reconstruction (see *e.g.* Morales-Castilla et al., 2015); however, phylogenetic proximity has
23 several desirable properties when working at large scales. Gerhold et al. (2015) made the point that
24 phylogenetic signal captures diversification of characters (large macro-evolutionary process), but not
25 necessarily community assembly (fine ecological process); Dormann et al. (2010) previously found very
26 similar conclusions. Interactions tend to reflect a phylogenetic signal because they have a conserved
27 pattern of evolutionary convergence that encompasses a wide range of ecological and evolutionary
28 mechanisms (Cavender-Bares et al., 2009; Mouquet et al., 2012), and - most importantly - retain this signal
29 even if it is obscured at the community scale due to *e.g.* local conditions (Hutchinson et al., 2017; Poisot &

30 Stouffer, 2018). Finally, species interactions at macro-ecological scales seem to respond mostly to
31 macro-evolutionary processes (Price, 2003); which is evidenced by the presence of conserved backbones in
32 food webs (Bramon Mora et al., 2018; Dalla Riva & Stouffer, 2016), strong evolutionary signature on prey
33 choice (Stouffer et al., 2012), and strong phylogenetic signature in food web intervality (Eklöf & Stouffer,
34 2016). Phylogenetic reconstruction has also previously been used within the context of ecological
35 networks, namely understanding ancestral plant-insect interactions (Braga et al., 2021). Taken together,
36 these considerations suggest that phylogenies can reliably be used to transfer knowledge on species
37 interactions.

38 [Figure 1 about here.]

39 In fig. 1, we provide a methodological overview based on learning the embedding of a metaweb of trophic
40 interactions for European mammals (known interactions; Maiorano et al., 2020a, 2020b) and, based on
41 phylogenetic relationships between mammals globally (*i.e.*, phylogenetic tree Upham et al., 2019), infer a
42 metaweb for the Canadian mammalian species pool (using only a species list *i.e.* we have no prior data on
43 species interaction data for Canada in this instance). Our case study shows that phylogenetic transfer
44 learning is an effective approach to the generation of probabilistic metawebs. This showcases that
45 although the components (species) that make up the Canadian and European communities may be
46 *minimally* shared (the overall species overlap is less than 4%), if the medium (proxy space) selected in the
47 transfer step is biologically plausible, we can still effectively learn from the known network and make
48 biologically relevant predictions of interactions. Indeed, as we detail in the results, when validated against
49 the known (but fractional) data of trophic interactions present between Canadian mammals, our model
50 achieves a predictive accuracy of approximately 91%.

51 **Method description**

52 The core point of our method is the transfer of knowledge of a known ecological network to predict
53 interactions between species for another location for which the network is unknown (or partially known)
54 and is summarized in the grey text boxes in fig. 1. The method we develop is, ecologically speaking, a
55 “black box,” *i.e.* an algorithm that can be understood mathematically, but whose component parts are not
56 always directly tied to ecological processes. There is a growing realization in machine learning that

57 (unintentional) black box algorithms are not necessarily a bad thing (Holm, 2019), as long as their
58 constituent parts can be examined (which is the case with our method). But more importantly, data hold
59 more information than we might think; as such, even algorithms that are disconnected from a model can
60 make correct guesses most of the time (Halevy et al., 2009); in fact, in an instance of ecological forecasting
61 of spatio-temporal systems, model-free approaches (*i.e.* drawing all of their information from the data)
62 outperformed model-informed ones (Perretti et al., 2013).

63 **Data used for the case study**

64 We use data from the European metaweb assembled by Maiorano et al. (2020a). This was assembled using
65 data extracted from scientific literature (including published papers, books, and grey literature) from the
66 last 50 years and includes all terrestrial tetrapods (mammals, breeding birds, reptiles and amphibians)
67 occurring on the European sub-continent (and Turkey) - with the caveat that only species introduced in
68 historical times and currently naturalized being included. The European metaweb was filtered using the
69 Global Biodiversity Information Facility (GBIF) taxonomic backbone (GBIF Secretariat, 2021) so as to
70 contain only terrestrial and semi-aquatic mammals. As all species had valid matches to the GBIF
71 taxonomy it was used as the backbone for the remaining reconciliation steps namely, the mammalian
72 consensus supertree by Upham et al. (2019) (which is used for the knowledge transfer step) and for the
73 Canadian species list—which was extracted from the International Union for Conservation of Nature
74 (IUCN) checklist, and corresponds to the same selection criteria that was applied by Maiorano et al.
75 (2020a) in the European metaweb. After taxonomic cleaning and reconciliation the European metaweb
76 has 260 species, and the Canadian species pool 163; of these, 17 (about 4% of the total) are shared, and 89
77 species from Canada (54%) had at least one congeneric species in Europe. The similarity for both species
78 pools predictably increases with higher taxonomic order, with 19% of shared genera, 47% of shared
79 families, and 75% of shared orders; for the last point, Canada and Europe each had a single unique order
80 (*Didelphimorphia* for Canada, *Erinaceomorpha* for Europe).

81 **Implementation and code availability**

82 The entire pipeline is implemented in *Julia* 1.6 (Bezanson et al., 2017) and is available under the
83 permissive MIT License at <https://osf.io/2zwqm/>. The taxonomic cleanup steps are done using GBIF .jl

84 (Dansereau & Poisot, 2021). The network embedding and analysis is done using `EcologicalNetworks.jl`
85 (Banville et al., 2021; Poisot et al., 2019). The phylogenetic simulations are done using `PhyloNetworks.jl`
86 (Solís-Lemus et al., 2017) and `Phylo.jl` (Reeve et al., 2016). A complete `Project.toml` file specifying the
87 full tree of dependencies is available alongside the code. This material also includes a fully annotated copy
88 of the entire code required to run this project (describing both the intent of the code and discussing some
89 technical implementation details), a vignette for every step of the process, and a series of Jupyter
90 notebooks with the text and code. The pipeline can be executed on a laptop in a matter of minutes, and
91 therefore does not require extensive computational power.

92 **Step 1: Learning the origin network representation**

93 The first step in transfer learning is to learn the structure of the original dataset. In order to do so, we rely
94 on an approach inspired from representational learning, where we learn a *representation* of the metaweb
95 (in the form of the latent subspaces), rather than a list of interactions (species *a* eats *b*). This approach is
96 conceptually different from other metaweb-scale predictions (e.g. Albouy et al., 2019), in that the metaweb
97 representation is easily transferable. Specifically, we use a Random Dot Product Graph model (hereafter
98 RDPG; S. J. Young & Scheinerman, 2007) to create a number of latent variables that can be combined into
99 an approximation of the network adjacency matrix. RDPG is known to capture the evolutionary backbone
100 of food webs (Dalla Riva & Stouffer, 2016), resulting in strong phylogenetic signal in RDPG results; in
101 other words, the latent variables of an RDPG can be mapped onto a phylogenetic tree, and
102 phylogenetically similar predators should share phylogenetically similar preys. In addition, recent
103 advances show that the latent variables produced this way can be used to predict *de novo* interactions.
104 Interestingly, the latent variables do not need to be produced by decomposing the network itself; in a
105 recent contribution, Runghen et al. (2021) showed that deep artificial neural networks are able to
106 reconstruct the left and right subspaces of an RDPG, in order to predict human movement networks from
107 individual/location metadata and opens up the possibility of using additional metadata as predictors.

108 The latent variables are created by performing a truncated Singular Value Decomposition (t-SVD; Halko et
109 al., 2011) on the adjacency matrix. SVD is an appropriate embedding of ecological networks, which has
110 recently been shown to both capture their complex, emerging properties (Strydom, Dalla Riva, et al., 2021)
111 and to allow highly accurate prediction of the interactions within a single network (Poisot, Ouellet, et al.,
112 2021). Under SVD, an adjacency matrix \mathbf{A} (where $\mathbf{A}_{m,n} \in \mathbb{B}$ where 1 indicates predation and 0 an absence

113 thereof) is decomposed into three components resulting in $\mathbf{A} = \mathbf{U}\mathbf{\Sigma}\mathbf{V}'$. Here, $\mathbf{\Sigma}$ is a $m \times n$ diagonal matrix
114 and contains only singular (σ) values along its diagonal, \mathbf{U} is a $m \times m$ unitary matrix, and \mathbf{V}' a $n \times n$
115 unitary matrix. Truncating the SVD removes additional noise in the dataset by omitting non-zero and/or
116 smaller σ values from $\mathbf{\Sigma}$ using the rank of the matrix. Under a t-SVD $\mathbf{A}_{m,n}$ is decomposed so that $\mathbf{\Sigma}$ is a
117 square $r \times r$ diagonal matrix (with $1 \leq r \leq r_{full}$ where r_{full} is the full rank of \mathbf{A} and r the rank at which we
118 truncate the matrix) containing only non-zero σ values. Additionally, \mathbf{U} is now an $m \times r$ semi unitary
119 matrix and \mathbf{V}' an $r \times n$ semi-unitary matrix.

120 The specific rank at which the SVD ought to be truncated is a difficult question. The purpose of SVD is to
121 remove the noise (expressed at high dimensions) and to focus on the signal (expressed at low dimensions).
122 In datasets with a clear signal/noise demarcation, a scree plot of $\mathbf{\Sigma}$ can show a sharp drop at the rank where
123 noise starts (Zhu & Ghodsi, 2006). Because the European metaweb is almost entirely known, the amount
124 of noise (uncertainty) is low; this is reflected in fig. 2 (left), where the scree plot shows no important drop,
125 and in fig. 2 (right) where the proportion of variance explained increases smoothly at higher dimensions.
126 For this reason, we default back to a threshold that explains 60% of the variance in the underlying data,
127 corresponding to 12 dimensions - *i.e.* a tradeoff between accuracy and a reduced number of features.

128 An RDPG estimates the probability of observing interactions between nodes (species) as a function of the
129 nodes' latent variables, and is a way to turn an SVD (which decompose one matrix into three) into two
130 matrices that can be multiplied to provide an approximation of the network. The latent variables used for
131 the RDPG, called the left and right subspaces, are defined as $\mathcal{L} = \mathbf{U}\sqrt{\mathbf{\Sigma}}$, and $\mathcal{R} = \sqrt{\mathbf{\Sigma}}\mathbf{V}'$ - using the full
132 rank of \mathbf{A} , $\mathcal{L}\mathcal{R} = \mathbf{A}$, and using any smaller rank results in $\mathcal{L}\mathcal{R} \approx \mathbf{A}$. Using a rank of 1 for the t-SVD
133 provides a first-order approximation of the network. One advantage of using an RDPG for the network
134 reconstruction rather than an SVD is that the number of components to estimate decreases; notably, one
135 does not have to estimate the singular values of the SVD. Furthermore, the two subspaces can be directly
136 multiplied to yield a network.

137 [Figure 2 about here.]

138 Because RDPG relies on matrix multiplication, the higher dimensions essentially serve to make specific
139 interactions converge towards 0 or 1; therefore, for reasonably low ranks, there is no guarantee that the
140 values in the reconstructed network will be within the unit range. In order to determine what constitutes
141 an appropriate threshold for probability, we performed the RDPG approach on the European metaweb,

142 and evaluated the probability threshold by treating this as a binary classification problem, specifically
143 assuming that both 0 and 1 in the European metaweb are all true. Given the methodological details given
144 in Maiorano et al. (2020a) and O'Connor et al. (2020), this seems like a reasonable assumption, although
145 one that does not hold for all metawebs. We used the thresholding approach presented in Poisot, Ouellet,
146 et al. (2021), and picked a cutoff that maximized Youden's J statistic (a measure of the informedness
147 (trust) of predictions; Youden (1950)); the resulting cutoff was 0.22, and gave an accuracy above 0.99. In
148 Supp. Mat. 1, we provide several lines of evidence that using the entire network to estimate the threshold
149 does not lead to overfitting; that using a subset of species would yield the same threshold; that decreasing
150 the quality of the original data by adding or removing interactions would minimally affect the predictive
151 accuracy of RDPG applied to the European metaweb; and that the networks reconstructed from artificially
152 modified data are reconstructed with the correct ecological properties.

153 The left and right subspaces for the European metaweb, accompanied by the threshold for prediction,
154 represent the knowledge we seek to transfer. In the next section, we explain how we rely on phylogenetic
155 similarity to do so.

156 **Steps 2 and 3: Transfer learning through phylogenetic relatedness**

157 In order to transfer the knowledge from the European metaweb to the Canadian species pool, we
158 performed ancestral character estimation using a Brownian motion model, which is a conservative
159 approach in the absence of strong hypotheses about the nature of phylogenetic signal in the network
160 decomposition (Litsios & Salamin, 2012). This uses the estimated feature vectors for the European
161 mammals to create a state reconstruction for all species (conceptually something akin to a trait-based
162 mammalian phylogeny using latent generality and vulnerability traits) and allows us to impute the
163 missing (latent) trait data for the Canadian species that are not already in the European network; as we are
164 focused on predicting contemporary interactions, we only retained the values for the tips of the tree. We
165 assumed that all traits (*i.e.* the feature vectors for the left and right subspaces) were independent, which is
166 a reasonable assumption as every trait/dimension added to the t-SVD has an *additive* effect to the one
167 before it. Note that the Upham et al. (2019) tree itself has some uncertainty associated to inner nodes of
168 the phylogeny. In this case study we have decided to not propagate this uncertainty as it would complexify
169 the process. The Brownian motion algorithm returns the *average* value of the trait, and its upper and
170 lower bounds. Because we do not estimate other parameters of the traits' distributions, we considered that

171 every species trait is represented as a uniform distribution between these bounds. The choice of the
172 uniform distribution was made because the algorithm returns a minimum and maximum point estimate
173 for the value, and given this information, the uniform distribution is the one with maximum entropy. Had
174 all mean parameters estimates been positive, the exponential distribution would have been an alternative,
175 but this is not the case for the subspaces of an RDPG. In order to examine the consequences of the choice
176 of distribution, we estimated the variance per latent variable per node to use a Normal distribution; as we
177 show in Supp. Mat. 2, this decision results in dramatically over-estimating the number and probability of
178 interactions, and therefore we keep the discussions in the main text to the uniform case. The inferred left
179 and right subspaces for the Canadian species pool ($\hat{\mathcal{L}}$ and $\hat{\mathcal{R}}$) have entries that are distributions,
180 representing the range of values for a given species at a given dimension. These objects represent the
181 transferred knowledge, which we can use for prediction of the Canadian metaweb.

182 **Step 4: Probabilistic prediction of the destination network**

183 The phylogenetic reconstruction of $\hat{\mathcal{L}}$ and $\hat{\mathcal{R}}$ has an associated uncertainty, represented by the breadth of
184 the uniform distribution associated to each of their entries. Therefore, we can use this information to
185 assemble a *probabilistic* metaweb in the sense of Poisot et al. (2016), *i.e.* in which every interaction is
186 represented as a single, independent, Bernoulli event of probability p .

187 [Figure 3 about here.]

188 Specifically, we have adopted the following approach. For every entry in $\hat{\mathcal{L}}$ and $\hat{\mathcal{R}}$, we draw a value from
189 its distribution. This results in one instance of the possible left ($\hat{\ell}$) and right (\hat{r}) subspaces for the
190 Canadian metaweb. These can be multiplied, to produce one matrix of real values. Because the entries in
191 $\hat{\ell}$ and \hat{r} are in the same space where \mathcal{L} and \mathcal{R} were originally predicted, it follows that the threshold ρ
192 estimated for the European metaweb also applies. We use this information to produce one random
193 Canadian metaweb, $N = \hat{\mathcal{L}}\hat{\mathcal{R}}' \geq \rho$. As we can see in (fig. 3), the European and Canadian metawebs are
194 structurally similar (as would be expected given the biogeographic similarities) and the two (left and right)
195 subspaces are distinct *i.e.* capturing predation (generality) and prey (vulnerability) latent traits.

196 Because the intervals around some trait values can be broad (in fact, probably broader than what they
197 would actually be, see *e.g.* Garland et al., 1999), we repeat the above process 2×10^5 times, which results in

198 a probabilistic metaweb P , where the probability of an interaction (here conveying our degree of trust that
199 it exists given the inferred trait distributions) is given by the number of times where it appears across all
200 random draws N , divided by the number of samples. An interaction with $P_{i,j} = 1$ means that these two
201 species were predicted to interact in all 2×10^5 random draws.

202 It must be noted that despite bringing in a large amount of information from the European species pool
203 and interactions, the Canadian metaweb has distinct structural properties. Following an approach similar
204 to Vermaat et al. (2009), we show in Supp. Mat. 3 that not only can we observe differences in the
205 multivariate space between the European and Canadian metawebs, we can also observe differences in the
206 same space between random subgraphs from these networks. These results line up with the studies
207 spatializing metawebs that have been discussed in the introduction: changes in the species pool are
208 driving local structural changes in the networks.

209 **Data cleanup, discovery, validation, and thresholding**

210 Once the probabilistic metaweb for Canada has been produced, we followed a number of data inflation
211 steps to finalize it. This step is external to the actual transfer learning framework but rather serves as a
212 way to augment and validate the predicted metaweb.

213 [Figure 4 about here.]

214 First, we extracted the network corresponding to the 17 species shared between the European and
215 Canadian pools and replaced these interactions with a probability of 0 (non-interaction) or 1 (interaction),
216 according to their value in the European metaweb. This represents a minute modification of the inferred
217 network (about 0.8% of all species pairs from the Canadian web), but ensures that we are directly re-using
218 knowledge from Europe.

219 Second, we looked for all species in the Canadian pool known to the Global Biotic Interactions (GloBI)
220 database (Poelen et al., 2014), and extracted their known interactions. Because GloBI aggregates observed
221 interactions, it is not a *networks* data source, and therefore the only information we can reliably extract
222 from it is that a species pair *was reported to interact at least once*. This last statement should yet be taken
223 with caution, as some sources in GloBI (e.g. Thessen & Parr, 2014) are produced through text analysis, and
224 therefore may not document direct evidence of the interaction. Nevertheless, should the predictive model

225 work, we would expect that a majority of interactions known to GloBI would also be predicted. We
226 retrieved 366 interactions between mammals from the Canadian species pool from GloBI, 33 of which
227 were not predicted by the model; this results in a success rate of 91%. After performing this check, we set
228 the probability of all interactions known to GloBI to 1.

229 Finally, we downloaded the data from Strong & Leroux (2014), who mined various literature sources to
230 identify trophic interactions in Newfoundland. This dataset documented 25 interactions between
231 mammals, only two of which were not part of our (Canada-level) predictions, resulting in a success rate of
232 92%. These two interactions were added to our predicted metaweb with a probability of 1. A comparison
233 of interaction densities for the inferred metaweb, and the GloBI and Newfoundland is shown in fig. 4 and a
234 table listing all interactions in the predicted Canadian metaweb can be found in the supplementary
235 material.

236 [Figure 5 about here.]

237 Because the confidence intervals on the inferred trait space are probably over-estimates, we decided to
238 apply a thresholding step to the interactions after data inflation (see fig. 5 showing the effect of varying the
239 cutoff on $P(i \rightarrow j)$). Cirtwill & Hambäck (2021) proposed a number of strategies to threshold probabilistic
240 networks. Their methodology assumes the underlying data to be tag-based sequencing, which represents
241 interactions as co-occurrences of predator and prey within the same tags; this is conceptually identical to
242 our Bernoulli-trial based reconstruction of a probabilistic network. We performed a full analysis of the
243 effect of various cutoffs, and as they either resulted in removing too few interactions, or removing enough
244 interactions that species started to be disconnected from the network, we set this threshold for a
245 probability equivalent to 0 to the largest possible value that still allowed all species to have at least one
246 interaction with a non-zero probability. The need for this slight deviation from the Cirtwill & Hambäck
247 (2021) methodology highlights the need for additional development on network thresholding.

248 **Results and discussion**

249 [Figure 6 about here.]

250 Using a transfer learning framework we were able to construct a probabilistic metaweb and (as per Dunne,
251 2006) is a list of potential interactions, meaning that they will not necessarily be realized wherever the two

252 species co-occur. The t-SVD embedding is able to learn relevant ecological features for the network. fig. 6
253 shows that the first rank correlates linearly with generality and vulnerability (Schoener, 1989), *i.e.* the
254 number of preys and predators for each species. Importantly, this implies that a rank 1 approximation
255 represents the configuration model for the metaweb, *i.e.* a set of random networks generated from a given
256 degree sequence (Park & Newman, 2004). Accounting for the probabilistic nature of the degrees, the rank
257 1 approximation also represents the *soft* configuration model (van der Hoorn et al., 2018). Both models are
258 maximum entropy graph models (Garlaschelli et al., 2018), with sharp (all network realizations satisfy the
259 specified degree sequence) and soft (network realizations satisfy the degree sequence on average) local
260 constraints, respectively. The (soft) configuration model is an unbiased random graph model widely used
261 by ecologists in the context of null hypothesis significance testing of network structure (*e.g.* Bascompte et
262 al., 2003) and can provide informative priors for Bayesian inference of network structure (*e.g.* J.-G. Young
263 et al., 2021). It is noteworthy that for this metaweb, the relevant information was extracted at the first
264 rank. Because the first rank corresponds to the leading singular value of the system, the results of fig. 6
265 have a straightforward interpretation: degree-based processes are the most important in structuring the
266 mammalian food web.

267 One important aspect in which Europe and Canada differ (despite their comparable bioclimatic
268 conditions) is the degree of the legacy of human impacts, which have been much longer in Europe.
269 Nenzén et al. (2014) showed that even at small scales (the Iberian peninsula), mammal food webs retain
270 the signal of both past climate change and human activity, even when this human activity was orders of
271 magnitude less important than it is now. Similarly, Yeakel et al. (2014) showed that changes in human
272 occupation over several centuries can lead to food web collapse. Megafauna in particular seems to be very
273 sensitive to human arrival (Pires et al., 2015). In short, there is well-substantiated support for the idea that
274 human footprint affects more than the risk of species extinction (Marco et al., 2018), and can lead to
275 changes in interaction structure.

276 Cirtwill et al. (2019) showed that network inference techniques based on Bayesian approaches would
277 perform far better in the presence of an interaction-level informative prior; the desirable properties of such
278 a prior would be that it is expressed as a probability, preferably representing a Bernoulli event, the value of
279 which would be representative of relevant biological processes (probability of predation in this case). We
280 argue that the probability returned at the very last step of our framework may serve as this informative
281 prior; indeed, the output of our analysis can be used in subsequent steps, also possibly involving expert

282 elicitation to validate some of the most strongly recommended interactions. One important *caveat* to keep
283 in mind when working with interaction inference is that interactions can never really be true negatives (in
284 the current state of our methodological framework and data collection limitations); this renders the task of
285 validating a model through the usual application of binary classification statistics very difficult (although
286 see Strydom, Catchen, et al., 2021 for a discussion of alternative suggestions). The other way through
287 which our framework can be improved is by substituting the predictors that are used for transfer. For
288 example, in the presence of information on species traits that are known to be predictive of species
289 interactions, one might want to rely on functional rather than phylogenetic distances – in food webs, body
290 size (and allometrically related variables) has been established as such a variable (Brose et al., 2006); the
291 identification of relevant functional traits is facilitated by recent methodological developments (Rosado et
292 al., 2013).

293 Finally, it should be noted that the framework we have presented is amenable to changes lending to
294 applicability to a broad range of potential scenarios. For example in this case study we have embedded the
295 original metaweb using t-SVD, because it lends itself to an RDPG reconstruction, which is known to
296 capture the consequences of evolutionary processes (Dalla Riva & Stouffer, 2016); this being said, there are
297 other ways to embed graphs (Arsov & Mirceva, 2019; Cai et al., 2017; Cao et al., 2019), which can be used
298 as alternatives. Regarding the transfer step it is possible to use distinct trees if working with distinct clades
299 (such as pollination networks) or an alternative measure of similarity (transfer medium) such as
300 information on foraging (Beckerman et al., 2006), cell-level mechanisms (Boeckaerts et al., 2021), or a
301 combination of traits and phylogenetic structure (Stock, 2021). Most importantly, although we focus on a
302 trophic system, it is an established fact that different (non-trophic) interactions do themselves interact with
303 and influence the outcome of trophic interactions (see *e.g.* Kawatsu et al., 2021; Kéfi et al., 2012). Future
304 development of metaweb inference techniques should cover the prediction of multiple interaction types.

305 **Acknowledgements:** We acknowledge that this study was conducted on land within the traditional
306 unceded territory of the Saint Lawrence Iroquoian, Anishinabewaki, Mohawk, Huron-Wendat, and
307 Omàmiwininiwak nations. TP, TS, DC, and LP received funding from the Canadian Institute for Ecology
308 & Evolution. FB is funded by the Institute for Data Valorization (IVADO). TS, SB, and TP are funded by a
309 donation from the Courtois Foundation. CB was awarded a Mitacs Elevate Fellowship no. IT12391, in
310 partnership with fRI Research, and also acknowledges funding from Alberta Innovates and the Forest
311 Resources Improvement Association of Alberta. M-JF acknowledges funding from NSERC Discovery

312 Grant and NSERC CRC. RR is funded by New Zealand's Biological Heritage Ngā Koiora Tuku Iho National
313 Science Challenge, administered by New Zealand Ministry of Business, Innovation, and Employment. BM
314 is funded by the NSERC Alexander Graham Bell Canada Graduate Scholarship and the FRQNT master's
315 scholarship. LP acknowledges funding from NSERC Discovery Grant (NSERC RGPIN-2019-05771). TP
316 acknowledges financial support from NSERC through the Discovery Grants and Discovery Accelerator
317 Supplement programs. MJF is supported by an NSERC PDF and an RBC Post-Doctoral Fellowship

318 **Conflict of interest:** The authors have no conflict interests to disclose

319 **Authors' contributions:** TS, SB, and TP designed the study and performed the analysis; GVDR, MF, and
320 RR provided additional feedback on the analyses. DC, BM, and FB helped with data collection. All
321 authors contributed to writing and editing the manuscript.

322 **Data availability:** All code and data used in this manuscript is publicly available and archived on OSF
323 <https://osf.io/2zwqm/> and is currently referenced in the manuscript.

324 **References**

- 325 Albouy, C., Archambault, P., Appeltans, W., Araújo, M. B., Beauchesne, D., Cazelles, K., Cirtwill, A. R.,
326 Fortin, M.-J., Galiana, N., Leroux, S. J., Pellissier, L., Poisot, T., Stouffer, D. B., Wood, S. A., & Gravel, D.
327 (2019). The marine fish food web is globally connected. *Nature Ecology & Evolution*, 3(8, 8),
328 1153–1161. <https://doi.org/10.1038/s41559-019-0950-y>
- 329 Arsov, N., & Mirceva, G. (2019, November 26). *Network Embedding: An Overview*.
330 <http://arxiv.org/abs/1911.11726>
- 331 Banville, F., Vissault, S., & Poisot, T. (2021). Mangal.jl and EcologicalNetworks.jl: Two complementary
332 packages for analyzing ecological networks in Julia. *Journal of Open Source Software*, 6(61), 2721.
333 <https://doi.org/10.21105/joss.02721>
- 334 Bascompte, J., Jordano, P., Melian, C. J., & Olesen, J. M. (2003). The nested assembly of plant-animal
335 mutualistic networks. *Proceedings of the National Academy of Sciences*, 100(16), 9383–9387.
336 <https://doi.org/10.1073/pnas.1633576100>
- 337 Beckerman, A. P., Petchey, O. L., & Warren, P. H. (2006). Foraging biology predicts food web complexity.
338 *Proceedings of the National Academy of Sciences*, 103(37), 13745–13749.

339 <https://doi.org/10.1073/pnas.0603039103>

340 Bezanson, J., Edelman, A., Karpinski, S., & Shah, V. (2017). Julia: A Fresh Approach to Numerical
341 Computing. *SIAM Review*, 59(1), 65–98. <https://doi.org/10.1137/141000671>

342 Boeckaerts, D., Stock, M., Criel, B., Gerstmans, H., De Baets, B., & Briers, Y. (2021). Predicting
343 bacteriophage hosts based on sequences of annotated receptor-binding proteins. *Scientific Reports*,
344 11(1, 1), 1467. <https://doi.org/10.1038/s41598-021-81063-4>

345 Braga, M. P., Janz, N., Nylin, S., Ronquist, F., & Landis, M. J. (2021). Phylogenetic reconstruction of
346 ancestral ecological networks through time for pierid butterflies and their host plants. *Ecology Letters*,
347 n/a(n/a). <https://doi.org/10.1111/ele.13842>

348 Bramon Mora, B., Gravel, D., Gilarranz, L. J., Poisot, T., & Stouffer, D. B. (2018). Identifying a common
349 backbone of interactions underlying food webs from different ecosystems. *Nature Communications*,
350 9(1), 2603. <https://doi.org/10.1038/s41467-018-05056-0>

351 Brose, U., Jonsson, T., Berlow, E. L., Warren, P., Banasek-Richter, C., Bersier, L.-F., Blanchard, J. L., Brey,
352 T., Carpenter, S. R., Blandenier, M.-F. C., Cushing, L., Dawah, H. A., Dell, T., Edwards, F.,
353 Harper-Smith, S., Jacob, U., Ledger, M. E., Martinez, N. D., Memmott, J., ... Cohen, J. E. (2006).
354 ConsumerResource Body-Size Relationships in Natural Food Webs. *Ecology*, 87(10), 2411–2417.
355 [https://doi.org/10.1890/0012-9658\(2006\)87%5B2411:CBRINF%5D2.0.CO;2](https://doi.org/10.1890/0012-9658(2006)87%5B2411:CBRINF%5D2.0.CO;2)

356 Cai, H., Zheng, V. W., & Chang, K. C.-C. (2017). *A Comprehensive Survey of Graph Embedding: Problems,*
357 *Techniques and Applications*. <http://arxiv.org/abs/1709.07604>

358 Cameron, E. K., Sundqvist, M. K., Keith, S. A., CaraDonna, P. J., Mousing, E. A., Nilsson, K. A., Metcalfe,
359 D. B., & Classen, A. T. (2019). Uneven global distribution of food web studies under climate change.
360 *Ecosphere*, 10(3), e02645. <https://doi.org/10.1002/ecs2.2645>

361 Cao, R.-M., Liu, S.-Y., & Xu, X.-K. (2019). Network embedding for link prediction: The pitfall and
362 improvement. *Chaos: An Interdisciplinary Journal of Nonlinear Science*, 29(10), 103102.
363 <https://doi.org/10.1063/1.5120724>

364 Cavender-Bares, J., Kozak, K. H., Fine, P. V. A., & Kembel, S. W. (2009). The merging of community
365 ecology and phylogenetic biology. *Ecology Letters*, 12(7), 693–715.
366 <https://doi.org/10.1111/j.1461-0248.2009.01314.x>

367 Cirtwill, A. R., Ekl, A., Roslin, T., Wootton, K., & Gravel, D. (2019). A quantitative framework for
368 investigating the reliability of empirical network construction. *Methods in Ecology and Evolution*, 0.
369 <https://doi.org/10.1111/2041-210X.13180>

370 Cirtwill, A. R., & Hambäck, P. (2021). Building food networks from molecular data: Bayesian or
371 fixed-number thresholds for including links. *Basic and Applied Ecology*, 50, 67–76.
372 <https://doi.org/10.1016/j.baae.2020.11.007>

373 Dalla Riva, G. V., & Stouffer, D. B. (2016). Exploring the evolutionary signature of food webs' backbones
374 using functional traits. *Oikos*, 125(4), 446–456. <https://doi.org/10.1111/oik.02305>

375 Dansereau, G., & Poisot, T. (2021). SimpleSDMLayers.jl and GBIF.jl: A Framework for Species
376 Distribution Modeling in Julia. *Journal of Open Source Software*, 6(57), 2872.
377 <https://doi.org/10.21105/joss.02872>

378 Dormann, C. F., Gruber, B., Winter, M., & Herrmann, D. (2010). Evolution of climate niches in European
379 mammals? *Biology Letters*, 6(2), 229–232. <https://doi.org/10.1098/rsbl.2009.0688>

380 Dunne, J. A. (2006). The Network Structure of Food Webs. In J. A. Dunne & M. Pascual (Eds.), *Ecological*
381 *networks: Linking structure and dynamics* (pp. 27–86). Oxford University Press.

382 Eklöf, A., & Stouffer, D. B. (2016). The phylogenetic component of food web structure and intervality.
383 *Theoretical Ecology*, 9(1), 107–115. <https://doi.org/10.1007/s12080-015-0273-9>

384 Garland, T., JR., Midford, P. E., & Ives, A. R. (1999). An Introduction to Phylogenetically Based Statistical
385 Methods, with a New Method for Confidence Intervals on Ancestral Values1. *American Zoologist*,
386 39(2), 374–388. <https://doi.org/10.1093/icb/39.2.374>

387 Garlaschelli, D., Hollander, F. den, & Roccaverde, A. (2018). Covariance structure behind breaking of
388 ensemble equivalence in random graphs. *Journal of Statistical Physics*, 173(3-4), 644–662.
389 <https://doi.org/10.1007/s10955-018-2114-x>

390 GBIF Secretariat. (2021). *GBIF Backbone Taxonomy*. <https://doi.org/10.15468/39omei>

391 Gerhold, P., Cahill, J. F., Winter, M., Bartish, I. V., & Prinzing, A. (2015). Phylogenetic patterns are not
392 proxies of community assembly mechanisms (they are far better). *Functional Ecology*, 29(5), 600–614.
393 <https://doi.org/10.1111/1365-2435.12425>

- 394 Halevy, A., Norvig, P., & Pereira, F. (2009). The Unreasonable Effectiveness of Data. *IEEE Intelligent*
395 *Systems*, 24(2), 8–12. <https://doi.org/10.1109/MIS.2009.36>
- 396 Halko, N., Martinsson, P. G., & Tropp, J. A. (2011). Finding Structure with Randomness: Probabilistic
397 Algorithms for Constructing Approximate Matrix Decompositions. *SIAM Review*, 53(2), 217–288.
398 <https://doi.org/10.1137/090771806>
- 399 Holm, E. A. (2019). In defense of the black box. *Science*, 364(6435), 26–27.
400 <https://doi.org/10.1126/science.aax0162>
- 401 Hortal, J., de Bello, F., Diniz-Filho, J. A. F., Lewinsohn, T. M., Lobo, J. M., & Ladle, R. J. (2015). Seven
402 Shortfalls that Beset Large-Scale Knowledge of Biodiversity. *Annual Review of Ecology, Evolution, and*
403 *Systematics*, 46(1), 523–549. <https://doi.org/10.1146/annurev-ecolsys-112414-054400>
- 404 Hutchinson, M. C., Cagua, E. F., & Stouffer, D. B. (2017). Cophylogenetic signal is detectable in pollination
405 interactions across ecological scales. *Ecology*, n/a–n/a. <https://doi.org/10.1002/ecy.1955>
- 406 Jordano, P. (2016a). Chasing Ecological Interactions. *PLOS Biol*, 14(9), e1002559.
407 <https://doi.org/10.1371/journal.pbio.1002559>
- 408 Jordano, P. (2016b). Sampling networks of ecological interactions. *Functional Ecology*, 30(12), 1883–1893.
409 <https://doi.org/10.1111/1365-2435.12763>
- 410 Kawatsu, K., Ushio, M., van Veen, F. J. F., & Kondoh, M. (2021). Are networks of trophic interactions
411 sufficient for understanding the dynamics of multi-trophic communities? Analysis of a tri-trophic
412 insect food-web time-series. *Ecology Letters*, 24(3), 543–552. <https://doi.org/10.1111/ele.13672>
- 413 Kéfi, S., Berlow, E. L., Wieters, E. A., Navarrete, S. A., Petchey, O. L., Wood, S. A., Boit, A., Joppa, L. N.,
414 Lafferty, K. D., Williams, R. J., Martinez, N. D., Menge, B. A., Blanchette, C. A., Iles, A. C., & Brose, U.
415 (2012). More than a meal... integrating non-feeding interactions into food webs: More than a meal
416 *Ecology Letters*, 15(4), 291–300. <https://doi.org/10.1111/j.1461-0248.2011.01732.x>
- 417 Litsios, G., & Salamin, N. (2012). Effects of Phylogenetic Signal on Ancestral State Reconstruction.
418 *Systematic Biology*, 61(3), 533–538. <https://doi.org/10.1093/sysbio/syr124>
- 419 Maiorano, L., Montemaggiore, A., Ficetola, G. F., O'Connor, L., & Thuiller, W. (2020a). TETRA-EU 1.0: A
420 species-level trophic metaweb of European tetrapods. *Global Ecology and Biogeography*, 29(9),
421 1452–1457. <https://doi.org/10.1111/geb.13138>

- 422 Maiorano, L., Montemaggiore, A., Ficetola, G. F., O'Connor, L., & Thuiller, W. (2020b). *Data from:*
423 *Tetra-EU 1.0: A species-level trophic meta-web of European tetrapods* (Version 3, pp. 16596876 bytes)
424 [Data set]. Dryad. <https://doi.org/10.5061/DRYAD.JM63XSJ7B>
- 425 Marco, M. D., Venter, O., Possingham, H. P., & Watson, J. E. M. (2018). Changes in human footprint drive
426 changes in species extinction risk. *Nature Communications*, 9(1), 4621.
427 <https://doi.org/10.1038/s41467-018-07049-5>
- 428 Morales-Castilla, I., Matias, M. G., Gravel, D., & Araújo, M. B. (2015). Inferring biotic interactions from
429 proxies. *Trends in Ecology & Evolution*, 30(6), 347–356.
430 <https://doi.org/10.1016/j.tree.2015.03.014>
- 431 Mouquet, N., Devictor, V., Meynard, C. N., Munoz, F., Bersier, L.-F., Chave, J., Coutron, P., Dalecky, A.,
432 Fontaine, C., Gravel, D., Hardy, O. J., Jabot, F., Lavergne, S., Leibold, M., Mouillot, D., Münkemüller,
433 T., Pavoine, S., Prinzing, A., Rodrigues, A. S. L., ... Thuiller, W. (2012). Ecophylogenetics: Advances
434 and perspectives. *Biological Reviews*, 87(4), 769–785.
435 <https://doi.org/10.1111/j.1469-185X.2012.00224.x>
- 436 Nenzén, H. K., Montoya, D., & Varela, S. (2014). The Impact of 850,000 Years of Climate Changes on the
437 Structure and Dynamics of Mammal Food Webs. *PLOS ONE*, 9(9), e106651.
438 <https://doi.org/10.1371/journal.pone.0106651>
- 439 O'Connor, L. M. J., Pollock, L. J., Braga, J., Ficetola, G. F., Maiorano, L., Martinez-Almoyna, C.,
440 Montemaggiore, A., Ohlmann, M., & Thuiller, W. (2020). Unveiling the food webs of tetrapods across
441 Europe through the prism of the Eltonian niche. *Journal of Biogeography*, 47(1), 181–192.
442 <https://doi.org/10.1111/jbi.13773>
- 443 Pan, S. J., & Yang, Q. (2010). A Survey on Transfer Learning. *IEEE Transactions on Knowledge and Data*
444 *Engineering*, 22(10), 1345–1359. <https://doi.org/10.1109/TKDE.2009.191>
- 445 Park, J., & Newman, M. E. J. (2004). Statistical mechanics of networks. *Physical Review E*, 70(6), 066117.
446 <https://doi.org/10.1103/PhysRevE.70.066117>
- 447 Perretti, C. T., Munch, S. B., & Sugihara, G. (2013). Model-free forecasting outperforms the correct
448 mechanistic model for simulated and experimental data. *Proceedings of the National Academy of*
449 *Sciences*, 110(13), 5253–5257. <https://doi.org/10.1073/pnas.1216076110>

- 450 Pires, M. M., Koch, P. L., Fariña, R. A., de Aguiar, M. A. M., dos Reis, S. F., & Guimarães, P. R. (2015).
451 Pleistocene megafaunal interaction networks became more vulnerable after human arrival.
452 *Proceedings of the Royal Society B: Biological Sciences*, 282(1814), 20151367.
453 <https://doi.org/10.1098/rspb.2015.1367>
- 454 Poelen, J. H., Simons, J. D., & Mungall, C. J. (2014). Global biotic interactions: An open infrastructure to
455 share and analyze species-interaction datasets. *Ecological Informatics*, 24, 148–159.
456 <https://doi.org/10.1016/j.ecoinf.2014.08.005>
- 457 Poisot, T., Belisle, Z., Hoebeke, L., Stock, M., & Szefer, P. (2019). EcologicalNetworks.jl - analysing
458 ecological networks. *Ecography*. <https://doi.org/10.1111/ecog.04310>
- 459 Poisot, T., Bergeron, G., Cazelles, K., Dallas, T., Gravel, D., MacDonald, A., Mercier, B., Violet, C., &
460 Vissault, S. (2021). Global knowledge gaps in species interaction networks data. *Journal of*
461 *Biogeography*, n/a(n/a). <https://doi.org/10.1111/jbi.14127>
- 462 Poisot, T., Cirtwill, A. R., Cazelles, K., Gravel, D., Fortin, M.-J., & Stouffer, D. B. (2016). The structure of
463 probabilistic networks. *Methods in Ecology and Evolution*, 7(3), 303–312.
464 <https://doi.org/10.1111/2041-210X.12468>
- 465 Poisot, T., Ouellet, M.-A., Mollentze, N., Farrell, M. J., Becker, D. J., Albery, G. F., Gibb, R. J., Seifert, S. N.,
466 & Carlson, C. J. (2021, May 31). *Imputing the mammalian virome with linear filtering and singular*
467 *value decomposition*. <http://arxiv.org/abs/2105.14973>
- 468 Poisot, T., & Stouffer, D. B. (2018). Interactions retain the co-phylogenetic matching that communities lost.
469 *Oikos*, 127(2), 230–238. <https://doi.org/10.1111/oik.03788>
- 470 Price, P. W. (2003). *Macroevolutionary theory on macroecological patterns*. Cambridge University Press.
- 471 Reeve, R., Leinster, T., Cobbold, C. A., Thompson, J., Brummitt, N., Mitchell, S. N., & Matthews, L. (2016,
472 December 8). *How to partition diversity*. <http://arxiv.org/abs/1404.6520>
- 473 Rosado, B. H. P., Dias, A., & de Mattos, E. (2013). Going Back to Basics: Importance of Ecophysiology
474 when Choosing Functional Traits for Studying Communities and Ecosystems. *Natureza &*
475 *Conservação Revista Brasileira de Conservação Da Natureza*, 11, 15–22.
476 <https://doi.org/10.4322/natcon.2013.002>
- 477 Runghen, R., Stouffer, D. B., & Dalla Riva, G. V. (2021). *Exploiting node metadata to predict interactions in*

478 *large networks using graph embedding and neural networks.*
479 <https://doi.org/10.1101/2021.06.10.447991>

480 Schoener, T. W. (1989). Food webs from the small to the large. *Ecology*, 70(6), 1559–1589.

481 Solís-Lemus, C., Bastide, P., & Ané, C. (2017). PhyloNetworks: A Package for Phylogenetic Networks.
482 *Molecular Biology and Evolution*, 34(12), 3292–3298. <https://doi.org/10.1093/molbev/msx235>

483 Stock, M. (2021). Pairwise learning for predicting pollination interactions based on traits and phylogeny.
484 *Ecological Modelling*, 14.

485 Stouffer, D. B., Sales-Pardo, M., Sirer, M. I., & Bascompte, J. (2012). Evolutionary Conservation of Species'
486 Roles in Food Webs. *Science*, 335(6075), 1489–1492. <https://doi.org/10.1126/science.1216556>

487 Strong, J. S., & Leroux, S. J. (2014). Impact of Non-Native Terrestrial Mammals on the Structure of the
488 Terrestrial Mammal Food Web of Newfoundland, Canada. *PLOS ONE*, 9(8), e106264.
489 <https://doi.org/10.1371/journal.pone.0106264>

490 Strydom, T., Catchen, M. D., Banville, F., Caron, D., Dansereau, G., Desjardins-Proulx, P., Forero-Muñoz,
491 N. R., Higinio, G., Mercier, B., Gonzalez, A., Gravel, D., Pollock, L., & Poisot, T. (2021). A roadmap
492 towards predicting species interaction networks (across space and time). *Philosophical Transactions of*
493 *the Royal Society B: Biological Sciences*, 376(1837), 20210063.
494 <https://doi.org/10.1098/rstb.2021.0063>

495 Strydom, T., Dalla Riva, G. V., & Poisot, T. (2021). SVD Entropy Reveals the High Complexity of Ecological
496 Networks. *Frontiers in Ecology and Evolution*, 9. <https://doi.org/10.3389/fevo.2021.623141>

497 Thessen, A. E., & Parr, C. S. (2014). Knowledge extraction and semantic annotation of text from the
498 encyclopedia of life. *PloS One*, 9(3), e89550.

499 Torrey, L., & Shavlik, J. (2010). Transfer learning. In *Handbook of research on machine learning*
500 *applications and trends: Algorithms, methods, and techniques* (pp. 242–264). IGI global.

501 Trøjelsgaard, K., & Olesen, J. M. (2016). Ecological networks in motion: Micro- and macroscopic
502 variability across scales. *Functional Ecology*, 30(12), 1926–1935.
503 <https://doi.org/10.1111/1365-2435.12710>

504 Upham, N. S., Esselstyn, J. A., & Jetz, W. (2019). Inferring the mammal tree: Species-level sets of
505 phylogenies for questions in ecology, evolution, and conservation. *PLOS Biology*, 17(12), e3000494.

506 <https://doi.org/10.1371/journal.pbio.3000494>

507 van der Hoorn, P., Lippner, G., & Krioukov, D. (2018). Sparse Maximum-Entropy Random Graphs with a
508 Given Power-Law Degree Distribution. *Journal of Statistical Physics*, 173(3-4), 806–844.
509 <https://doi.org/10.1007/s10955-017-1887-7>

510 Vermaat, J. E., Dunne, J. A., & Gilbert, A. J. (2009). Major dimensions in food-web structure properties.
511 *Ecology*, 90(1), 278–282. <http://www.ncbi.nlm.nih.gov/pubmed/19294932>

512 Yeakel, J. D., Pires, M. M., Rudolf, L., Dominy, N. J., Koch, P. L., Guimarães, P. R., & Gross, T. (2014).
513 Collapse of an ecological network in Ancient Egypt. *PNAS*, 111(40), 14472–14477.
514 <https://doi.org/10.1073/pnas.1408471111>

515 Youden, W. J. (1950). Index for rating diagnostic tests. *Cancer*, 3(1), 32–35.
516 [https://doi.org/10.1002/1097-0142\(1950\)3:1%3C32::AID-CNCR2820030106%3E3.0.CO;2-3](https://doi.org/10.1002/1097-0142(1950)3:1%3C32::AID-CNCR2820030106%3E3.0.CO;2-3)

517 Young, J.-G., Cantwell, G. T., & Newman, M. E. J. (2021). Bayesian inference of network structure from
518 unreliable data. *Journal of Complex Networks*, 8(6). <https://doi.org/10.1093/comnet/cnaa046>

519 Young, S. J., & Scheinerman, E. R. (2007). Random Dot Product Graph Models for Social Networks. In A.
520 Bonato & F. R. K. Chung (Eds.), *Algorithms and Models for the Web-Graph* (pp. 138–149). Springer.
521 https://doi.org/10.1007/978-3-540-77004-6_11

522 Zhu, M., & Ghodsi, A. (2006). Automatic dimensionality selection from the scree plot via the use of profile
523 likelihood. *Computational Statistics & Data Analysis*, 51(2), 918–930.
524 <https://doi.org/10.1016/j.csda.2005.09.010>

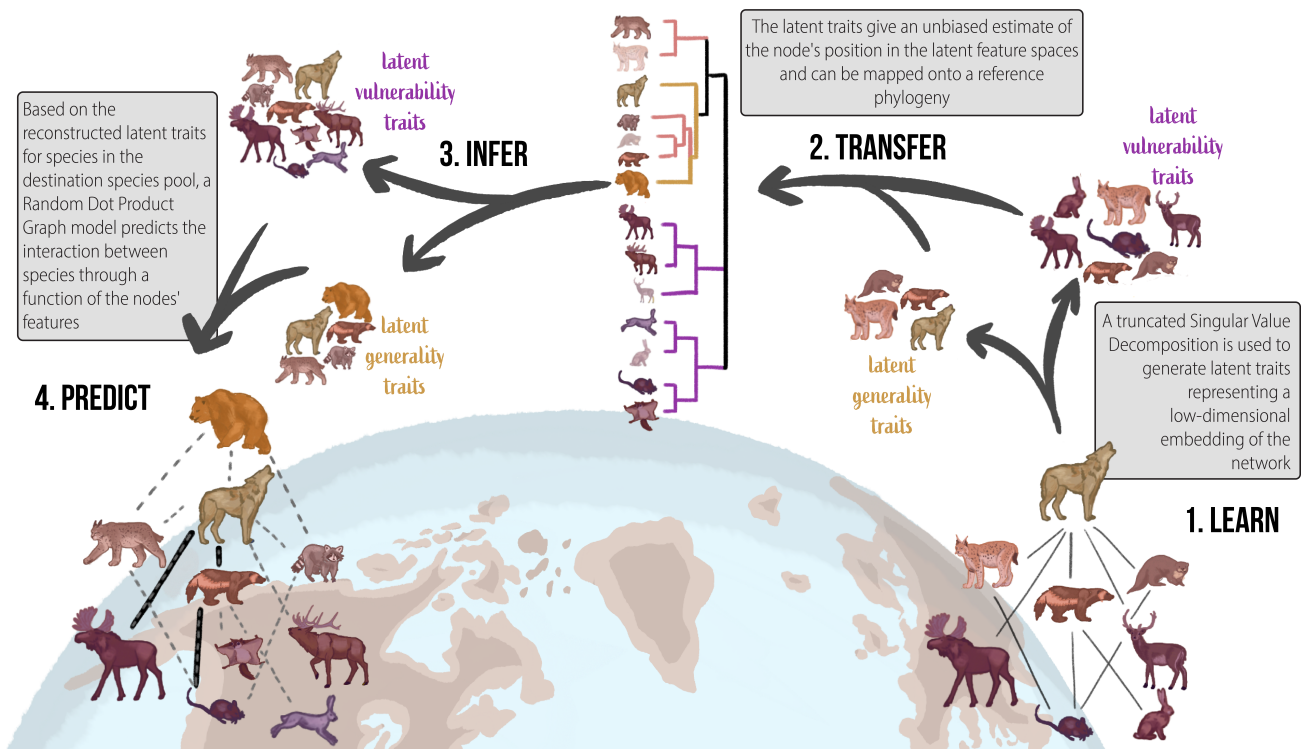


Figure 1: Overview of the phylogenetic transfer learning (and prediction) of species interactions networks. Starting from an initial, known, network, we learn its representation through a graph embedding step (here, a truncated Singular Value Decomposition; Step 1), yielding a series of latent traits (latent vulnerability traits are more representative of species at the lower trophic-level and latent generality traits are more representative of species at higher trophic-levels; *sensu* Schoener (1989)); second, for the destination species pool, we perform ancestral character estimation using a phylogeny (here, using a Brownian model for the latent traits; Step 2); we then sample from the reconstructed distribution of latent traits (Step 3) to generate a probabilistic metaweb at the destination (here, assuming a uniform distribution of traits), and threshold it to yield the final list of interactions (Step 4).

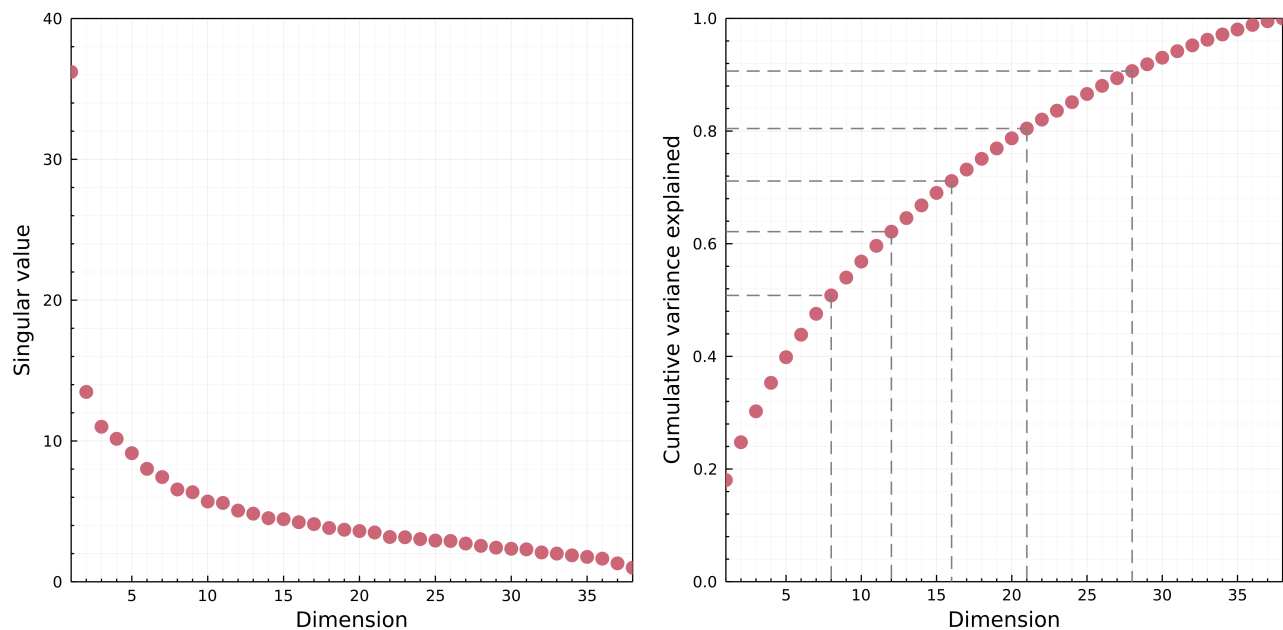


Figure 2: Left: representation of the scree plot of the singular values from the t-SVD on the European metaweb. The scree plot shows no obvious drop in the singular values that may be leveraged to automatically detect a minimal dimension for embedding, after *e.g.* Zhu & Ghodsi (2006). Right: cumulative fraction of variance explained by each dimension up to the rank of the European metaweb. The grey lines represent cutoffs at 50, 60, ..., 90% of variance explained. For the rest of the analysis, we reverted to an arbitrary threshold of 60% of variance explained, which represented a good tradeoff between accuracy and reduced number of features.

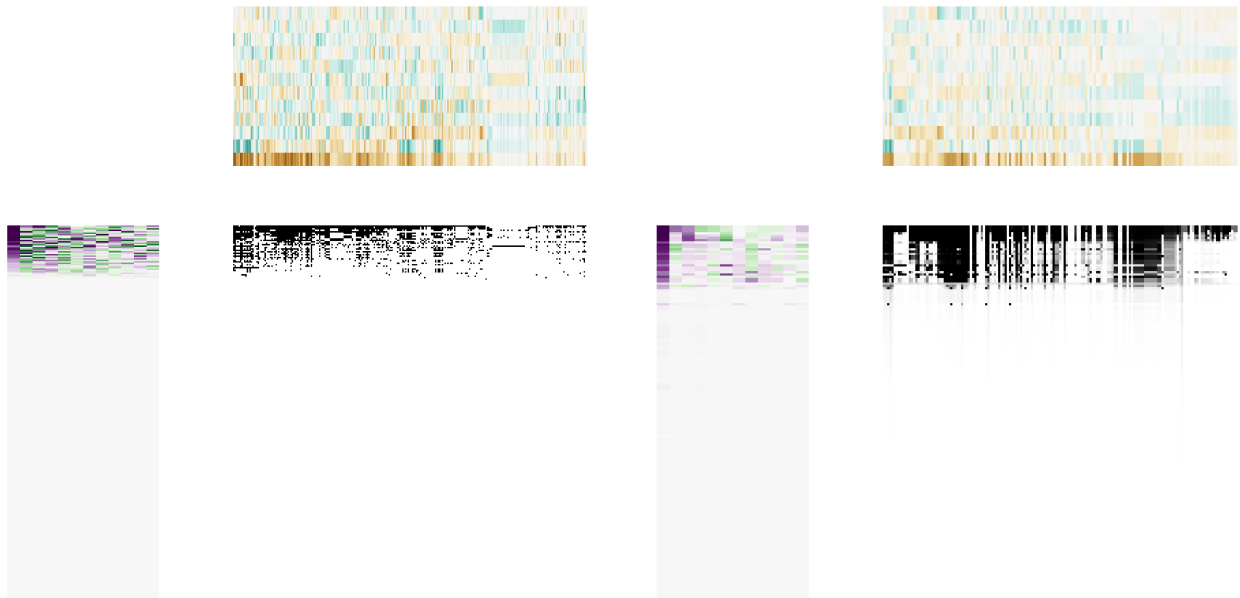


Figure 3: Visual representation of the left (green/purple; left-side matrix) and right (green/brown; top matrix) subspaces, alongside the adjacency matrix of the food web they encode (greyscale). Where the color saturation is the magnitude of the latent trait value. The European metaweb is on the left, and the imputed Canadian metaweb (before data inflation) on the right. This figure illustrates how much structure the left subspace captures. As we show in fig. 6, the species with a value of 0 in the left subspace are species without any prey.

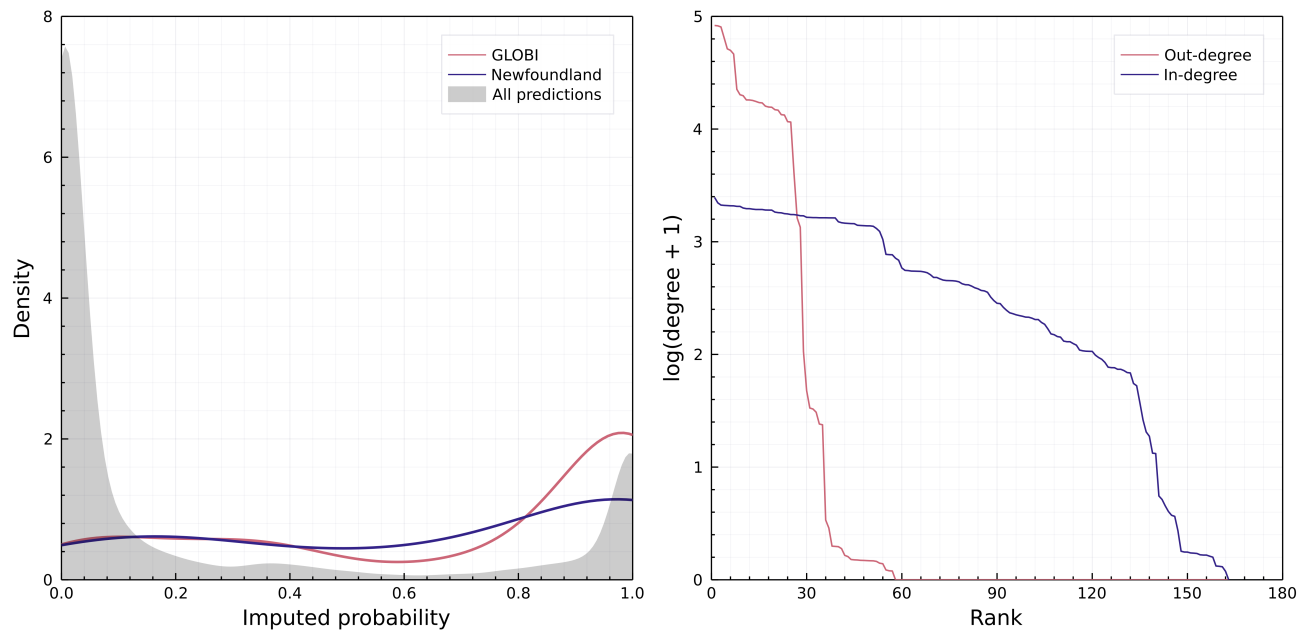


Figure 4: Left: comparison of the probabilities of interactions assigned by the model to all interactions (grey curve), the subset of interactions found in GloBI (red), and in the Strong & Leroux (2014) Newfoundland dataset (blue). The model recovers more interactions with a low probability compared to data mining, which can suggest that collected datasets are biased towards more common or easy to identify interactions. Right: distribution of the in-degree and out-degree of the mammals from Canada in the reconstructed metaweb, where the rank is the maximal number of linearly independent columns (interactions) in the metaweb. This figure describes a flat, relatively short food web, in which there are few predators but a large number of preys.

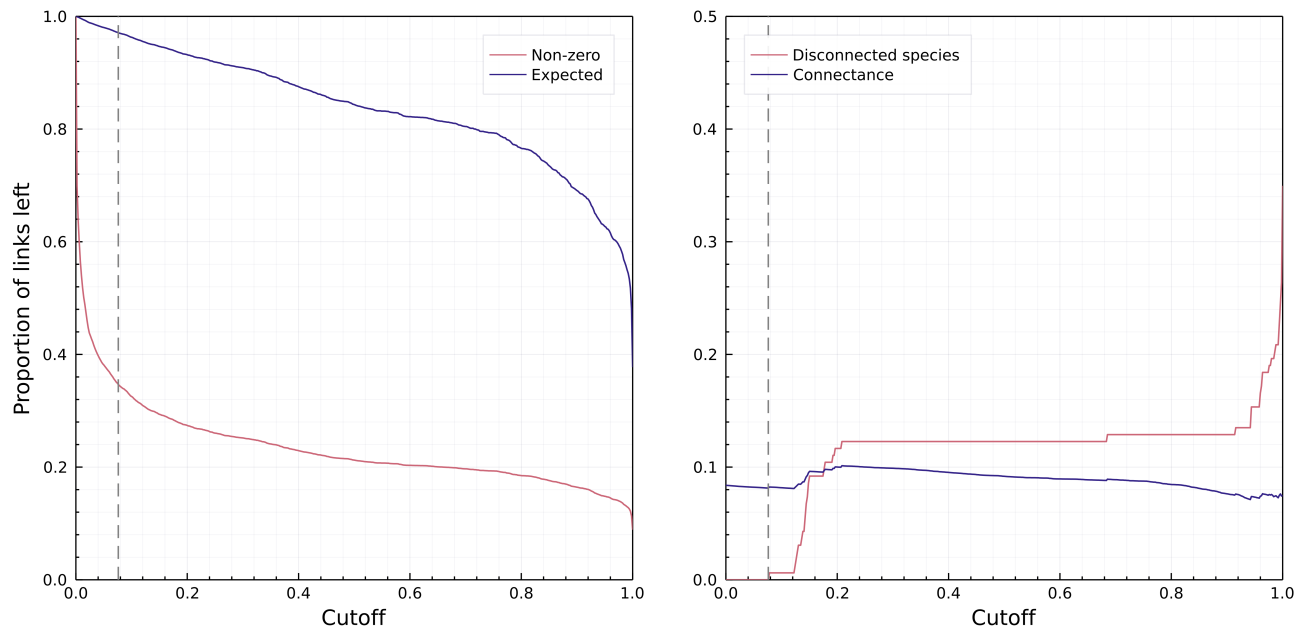


Figure 5: Left: effect of varying the cutoff for probabilities to be considered non-zero on the number of unique links and on \hat{L} , the probabilistic estimate of the number of links assuming that all interactions are independent. Right: effect of varying the cutoff on the number of disconnected species, and on network connectance. In both panels, the grey line indicates the cutoff $P(i \rightarrow j) \approx 0.08$ that resulted in the first species losing all of its interactions.

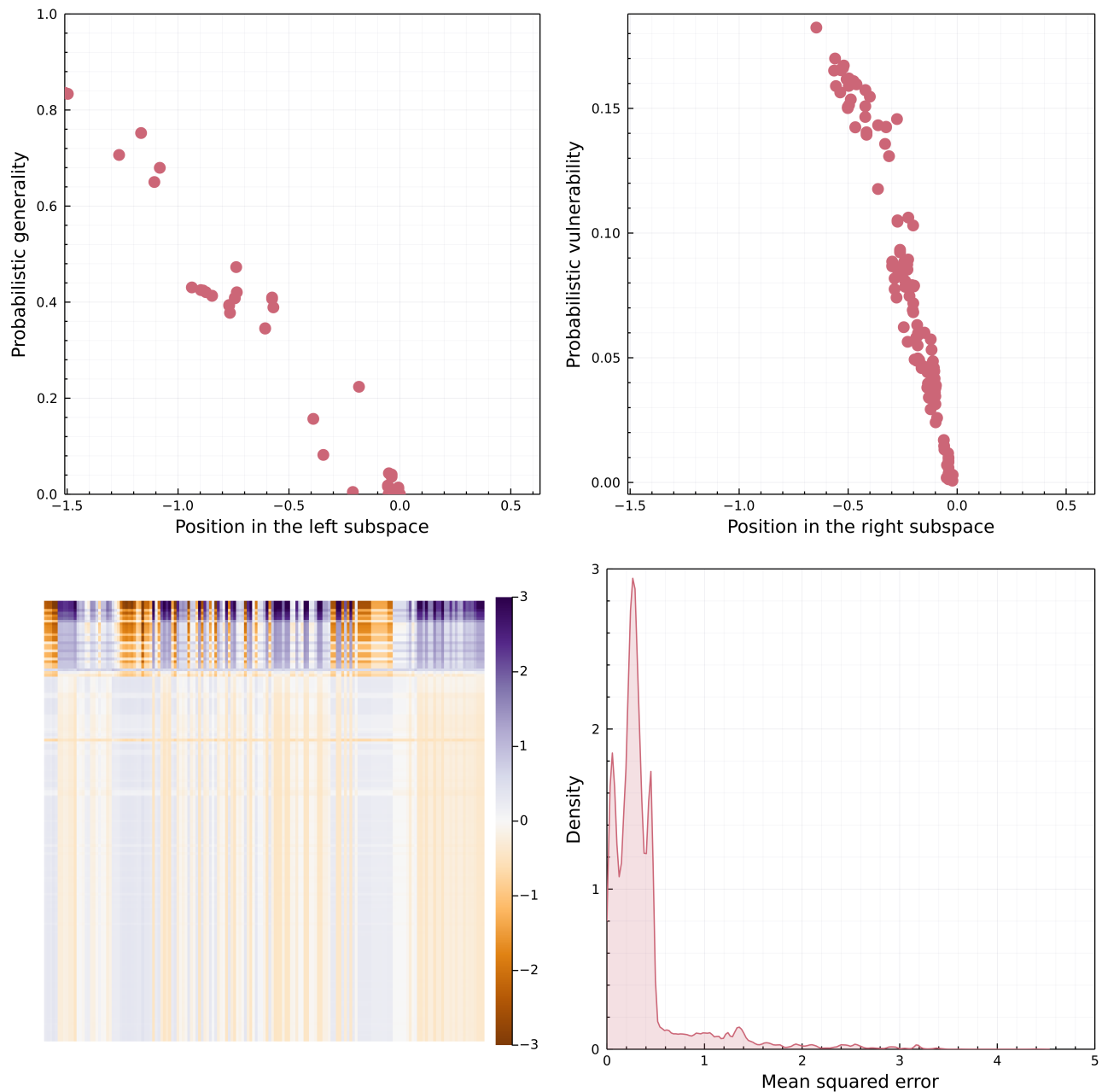


Figure 6: Top: biological significance of the first dimension. Left: there is a linear relationship between the values on the first dimension of the left subspace and the generality, *i.e.* the relative number of preys, *sensu* Schoener (1989). Species with a value of 0 in this subspace are at the bottom-most trophic level. Right: there is, similarly, a linear relationship between the position of a species on the first dimension of the right subspace and its vulnerability, *i.e.* the relative number of predators. Taken together, these two figures show that the first-order representation of this network would capture its degree distribution. Bottom: topological consequences of the first dimension. Left: differences in the z-scores of the actual configuration and the prediction based only on the first dimension (with a deeper saturation indicating a bigger difference in scores). Right: distribution of the differences in the left panel.